

## N O T I C E

THIS DOCUMENT HAS BEEN REPRODUCED FROM  
MICROFICHE. ALTHOUGH IT IS RECOGNIZED THAT  
CERTAIN PORTIONS ARE ILLEGIBLE, IT IS BEING RELEASED  
IN THE INTEREST OF MAKING AVAILABLE AS MUCH  
INFORMATION AS POSSIBLE

"Made available under NASA sponsorship  
in the interest of early and wide dis-  
semination of Earth Resources Survey  
Program information and without liability  
for any use made thereof."

(E80-10152) REMOTE SENSING ANALYSIS OF  
WATER QUALITY AND THE ENTRAPMENT ZONE IN THE  
SAN FRANCISCO BAY AND DELTA Final Report,  
15 Mar. 1978 14 Aug. 1979 (California  
Univ.) 40 p HC A03/MF A01

N80-25734

Unclas  
00152

CSCL 13B G3/43

# SCIENCES LABORATORY

80-10152.  
CR-163169

## REMOTE SENSING ANALYSIS OF WATER QUALITY AND THE ENTRAPMENT ZONE IN THE SAN FRANCISCO BAY AND DELTA

Professor Robert N. Colwell, Principal Investigator  
Professor Allen W. Knight, Co-Investigator  
Dr. Siamak Khorram, Principal Scientist and Project Manager

A report of research performed by scientists of two campuses of  
the University of California (Berkeley and Davis) under NASA  
Grant NSG-5256 and Water Resources Center Project  
UCAL-WRC-W561

Final Report  
14 August 1979  
Space Sciences Laboratory  
Series 20, Issue 42

UNIVERSITY OF CALIFORNIA, BERKELEY

REMOTE SENSING ANALYSIS OF WATER QUALITY  
AND THE ENTRAPMENT ZONE IN THE  
SAN FRANCISCO BAY AND DELTA

Professor Robert N. Colwell, Principal Investigator  
Professor Allen W. Knight, Co-Investigator  
Dr. Siamak Khorram, Principal Scientist and Project Manager

A report of research performed by scientists of two campuses of  
the University of California (Berkeley and Davis) under NASA  
Grant NSG-5256 and Water Resources Center Project  
UCAL-WRC-W561

Final Report  
14 August 1979

Space Sciences Laboratory  
Series 20, Issue 42

University of California

Original photography may be purchased from  
EROS Data Center

Spokane Falls, WA 57198

## PREFACE

The quality of water in the Delta, and the effect that various uses might have on that water quality, is a matter of great interest to a number of state, federal, and local government agencies. Of particular interest is an area at approximately the point where salty tidal water moving up the Delta from San Francisco Bay meets fresh water flowing to the Bay from the Sacramento and San Joaquin rivers.

Known as the region of "high biological activity" because of its abundance of fish and plant life, this shifting, constantly changing area is difficult to map and monitor. In the fall of 1978, a team of University of California Scientists was asked to determine if remote sensing, combined with information gathered on-site, could be used to measure water quality in San Francisco Bay and the Delta, and to locate this region of high biological activity.

Data was collected on September 14, 1978 by means of an Ocean Color Scanner (OCS) flown on a NASA U-2 plane at an altitude of 65,000 feet. The aircraft also took conventional color and color infrared photographs. Water quality samples were taken simultaneously from boats at 29 pre-determined sites in the study area. Statistical comparisons were then made of the data, parameter estimation models were developed and tested, and separate color-coded maps were prepared for each of the four water quality parameters being analyzed.

As shown in the report, the area of high biological activity was clearly discernible on computer-enhanced imagery of the OCS data. The area could not be consistently identified by high quality aerial photography taken with either conventional color film or infrared color film.

The scientists consider the preliminary results of the study highly promising and believe remote sensing will be useful in monitoring water quality in San Francisco Bay and the Delta.

## Table of Contents

|  | <u>Page</u> |
|--|-------------|
| Preface  | i           |
| Table of Contents  | ii          |
| List of Tables   | iii         |
| List of Illustrations  | iv          |
| 1.0 Introduction   | 1           |
| 2.0 Technical Approach   | 3           |
| 3.0 Methodology  | 4           |
| 3.1 Collection and Laboratory Analysis<br>of Water Quality Samples                                       | 4           |
| 3.2 Acquisition and Analysis of the<br>Ocean Color Scanner (OCS) data                                    | 4           |
| 3.3 Development of Regression Models for<br>Estimating Water Quality Parameters<br>from OCS Data         | 9           |
| 3.4 Acquisition and Analysis of Landsat<br>Multispectral Scanner Data                                    | 9           |
| 3.5 Development of Regression Models for<br>Estimating Water Quality Parameters<br>from Landsat MSS Data | 11          |
| 3.6 Applications of Regression Models Based<br>on the OCS or Landsat Data to the Entire<br>Study Area    | 11          |
| 4.0 Results  | 12          |
| 4.1 Regression Models Based on the OCS Data  | 12          |
| 4.2 Regression Models Based on Landsat<br>MSS Data   | 17          |
| 5.0 Discussion   | 18          |
| 6.0 Conclusion   | 29          |
| Acknowledgements   | 31          |
| References   | 32          |

### List of Tables

| <u>Table</u> |  | <u>Page</u> |
|--------------|--|-------------|
| 1            | Peak wavelength and ranges for the four OCS channels used in this study and wavelength ranges for the four Landsat MSS bands.  | 8           |
| 2            | The results of laboratory analysis for water quality samples collected on September 14, 1978.  | 15          |
| 3            | Correlation Coefficients (R) and "F" values relating remotely sensed data to "ground truth" for the four water quality parameters estimated using the regression models on Ocean Color Scanner (OCS) and Landsat data. | 27          |

## List of Illustrations

| <u>Figure</u> |   | <u>Page</u> |
|---------------|---|-------------|
| 1             | Location of water quality sample sites in the Delta Region. The sites were numbered 1 to 29 from left to right.             | 5           |
| 2             | Display of digital OCS data in Channel 10 prior to rectification of the dropout regions.                                    | 13          |
| 3             | Display of digital OCS data in Channel 10 after rectification of the dropout regions and masking.                           | 13          |
| 4             | Landsat raw data color composite of Bands 4, 5, and 7 of the study area after rectifying the bad data lines.                | 14          |
| 5             | Salinity distribution as derived from OCS data for the Delta region; San Pablo Bay is on left.                              | 19          |
| 6             | Chlorophyll distribution as derived from OCS data for the Delta region; San Pablo Bay is on left.                           | 20          |
| 7             | Suspended solids distribution as derived from OCS data in the Delta region; San Pablo Bay is on left.                       | 21          |
| 8             | Turbidity distribution as derived from OCS data for the Delta region; San Pablo Bay is on left.                             | 22          |
| 9             | Salinity distribution as derived from the enhanced Landsat MSS data for the Delta region; San Pablo Bay is on left.         | 23          |
| 10            | Chlorophyll distribution as derived from the enhanced Landsat MSS data for the Delta region; San Pablo Bay is on left.      | 24          |
| 11            | Suspended solids distribution as derived from the enhanced Landsat MSS data for the Delta region; San Pablo Bay is on left. | 25          |
| 12            | Turbidity distribution as derived from the enhanced Landsat MSS data for the Delta region; San Pablo Bay is on left.        | 26          |

ORIGINAL PAGE IS  
OF POOR QUALITY

## 1.0 INTRODUCTION

Water demand in the State of California is constantly increasing with the increase in population, improvement in the standard of living and the expansion of industry. The San Francisco Bay and the associated delta that is formed by the confluence of the Sacramento and San Joaquin Rivers constitute one of California's most important aquatic resources. Because of this area's wealth of industrial, recreational and aesthetic resources, there are many conflicting proposals on how it might best be used. There also are conflicting opinions on the extent to which any given use might affect water quality throughout the area. Within this study area there is a "region of high biological activity" because physical forces are such that there is an upwelling of the heavier salt water, which in turn stimulates a downwelling of fresh water and a consequent circulation of water currents and their associated nutrients.

Regions of high turbidity and high suspended solids appear to be a persistent feature of moderately stratified estuaries (Mead 1972). A region of maximum turbidity was measured as early as 1893 in the Gironde - Garonne Estuary of France (Glandeaud, 1939). Recently several investigators, through the use of conventional ground survey techniques, have reported a region of high turbidity in many estuaries of northern Europe, British Guiana and the United States (Postma, 1967; Schubel, 1968; Mead, 1968; and Arthur, 1975, 1977). Other investigators have noted a region of greatest suspended sediment accumulation in Thames Estuary (Inglis and Allen, 1957). Peterson et al (1975) have suggested that the water column in the non-tidal current null zone in northern San Francisco Bay experiences the longest advective replacement time relative to other portions and the estuary, which may affect the planktonic community.

In a few instances (Barker, 1975; Brooks, 1975, Scherz et al, 1975; Rogers et al, 1975; Johnson, 1976; and McKeon and Rogers, 1976) remote sensing data derived from multi-spectral scanners also have been used for the purpose of water quality mapping. Draeger, et al (1974) provide a comprehensive review of the literature pertaining to the use of remotely sensed data for measuring and monitoring water quality. That review in conjunction with cooperative studies with the Department of Water Resources concluded that remotely sensed



data have the potential for measuring water quality parameters in an operational mode if 1.) surface and airborne measurements are taken simultaneously, 2.) sensors are calibrated for accurately and consistently relating reflectance characteristics of the water quality parameter to image signature, and 3.) robust models are developed and tested allowing water surface reflectance values to be correlated to surface and subsurface water quality parameters. This study constitutes the first instance in which there has been a concerted effort to use remote sensing to locate the region of highest biological activity and map the associated water quality parameters in an operational mode.

As an integral part of this project, water quality data were collected by means of surface monitoring programs between 1968 and 1973. This collection effort was performed by personnel of the Department of Land, Air, and Water Resources from the Davis campus of the University of California under the direction of Dr. Allen W. Knight. It demonstrated that concentrations of phytoplankton, chlorophyll, particulate organic nitrogen and phosphate, as well as inorganic suspended solids, and overall turbidity, were significantly higher in the "region of high biological activity" than in the adjacent upstream and downstream areas. Location of this region may thus have important effects upon the Delta fisheries, whose contribution to the economy of the area is officially estimated to exceed \$10 million annually. This "region of high biological activity" (often referred to as the "Entrapment Zone") may be characterized by quantifying, comparing, and monitoring suspended solids, chlorophyll, turbidity, and conductivity parameters along the longitudinal axis of the estuary. The usefulness of remote sensing for mapping these important water quality parameters has been examined and demonstrated under this investigation.

The objective of this research effort was to investigate the use of remotely sensed data, combined with in situ data, for assessing water quality parameters and for locating the "region of high biological activity" within the San Francisco Bay Delta. The water quality parameters of interest included suspended solids, chlorophyll concentration, turbidity, and electrical conductivity

(salinity) The remote sensing data included the Ocean Color Scanner (OCS) data and color infrared photography, both of which were obtained from a NASA U-2 aircraft, and Landsat multispectral scanner (MSS) data.

## 2.0 TECHNICAL APPROACH

The general approach involved simultaneous acquisition not only of all remotely sensed data but also of water quality samples from boats. The simultaneous collection of water quality samples and remotely sensed data was coordinated and conducted by both the Berkeley and Davis teams. Regression models were then developed between each of the water quality measurements and the remotely sensed data. These models were developed in two stages: 1) between the water quality measurements and OCS data, and 2) between the water quality measurements and Landsat MSS data. The regression models were then extended to the entire study area for use in mapping of the water quality parameters of interest. The methodology is divided into the following six sections:

1. Collection and laboratory analysis of water quality samples.
2. Acquisition and analysis of the Ocean Color Scanner (OCS) data.
3. Development of regression models for estimating water quality parameters from OCS data.
4. Acquisition and analysis of Landsat Multispectral Scanner (MSS) data.
5. Development of regression models for estimating water quality parameters from Landsat MSS data.
6. Application to the entire study area of regression models based on the OCS and Landsat data.

### 3.0 METHODOLOGY

#### 3.1 Collection and Laboratory Analysis of Water Quality Samples:

On September 14, 1978, samples of the four selected water quality parameters were collected at 29 pre-determined sites in the San Francisco Bay-Delta Region. These water quality parameters measured on the 29 sample sites included salinity, turbidity, and suspended solids. In addition, chlorophyll concentration was measured on nine of the 29 sites. These samples as shown in Figure 1 were distributed throughout the Delta. The chlorophyll data were only collected on the first nine sites as the sample boats progressed from San Pablo Bay toward the Delta region.

Water samples used for determining suspended solids were collected through a weighted hose. Samples were iced in the field and taken to the laboratory for analysis. In the laboratory, suspended matters were collected by vacuum filtration on pre-weighed 0.45 $\mu$  filters, dried at 105°C, and reweighed on an analytical balance. Chlorophyll samples were collected by vacuum filtration on glass fiber filters, pre-treated with MgCO<sub>3</sub> suspension, and analyzed by the fluorometric method. Turbidity and salinity were determined in situ by a turbidity meter instrument and a refractometer, respectively.

#### 3.2 Acquisition and Analysis of the Ocean Color Scanner (OCS) Data

The ocean color scanner is a ten channel line scanning radiometer having a 90° total field of view and a 3.5 milliradian spatial resolution. This scanner was flown on a NASA U-2 aircraft at an altitude of 65,000 feet over the study area on September 14, 1978. The calibrated computer compatible tapes of the OCS data were obtained from NASA-Goddard Space Flight Center (GSFC). The following procedure was used in processing and analyzing the OCS data.

▲ N

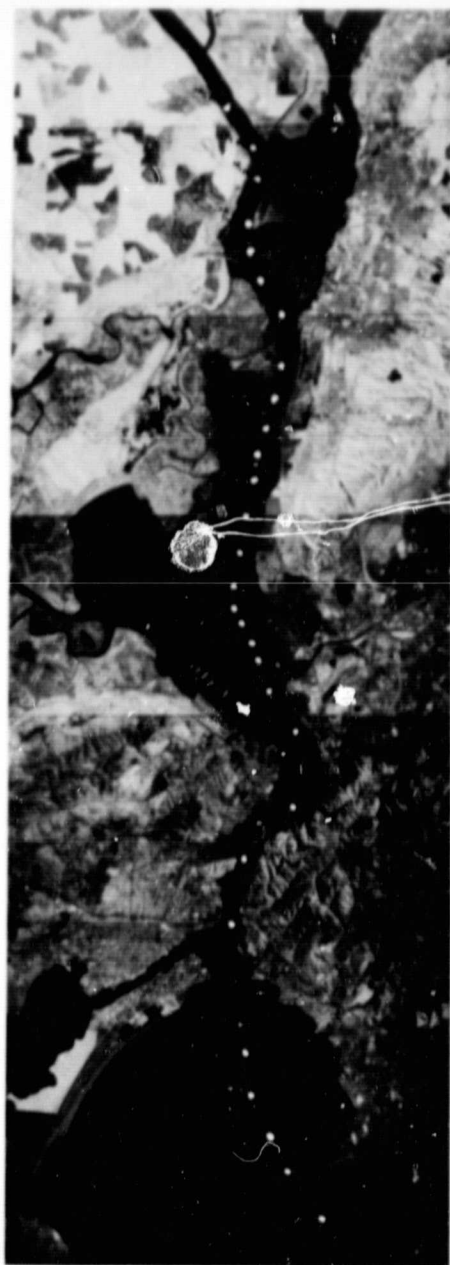


Figure 1. Location of water quality sample sites in the Delta Region.  
The sites were numbered 1 to 29 from left to right.

### 3.2.1 Data Reformatting

An algorithm was developed and applied for reformatting the OCS data from the GSFC format to the format of the Remote Sensing Research Program (RSRP) data processing system.

### 3.2.2 Bad Data Rectification

The OCS data contained a large number of bad data lines (referred to in this report as "dropouts"). These dropouts resulted from the malfunctioning of the digitizer on the scanner at the time of data acquisition.

Two procedures for replacing the bad lines were used. Procedure One was used to replace data line dropouts not exceeding three consecutive lines. This procedure was based on a linear interpolation of the data from reliable data of a line above and below the dropout region. In this procedure, we simply replaced the dropout lines, pixel-by-pixel, with the linearly interpolated values between the lines immediately above and below the dropouts. Procedure Two was used to eliminate dropout regions exceeding three consecutive lines. This situation occurred on the average of once per one hundred scan lines in each band. Procedure Two utilized RSRP developed software to create data lines in the dropout regions. This replacement was accomplished as follows: For each band to be corrected (i.e. dropout regions replaced) which we will call "Band A", we determined which of the available bands with a different dropout pattern (i.e. "Band B") was most highly correlated with "Band A". For each set of dropout regions in "Band A", we located the nearest scan lines above and below the dropout area which had reliable data in both "Band A" and "Band B". On the basis of these two lines, we constructed a table containing the transformations from corresponding lines in "Band B". None of the 29 sample sites corresponded to areas of large data dropouts on the spectral channels used.

### 3.2.3 OCS Channel Selection

The OCS data consisted of six useable channels. Channels 1, 2, 8 and 9 were not used. Channels 1 and 2 were deemed inappropriate data for water quality studies; Channel 8 was not acquired over the study area; and Channel 9 was designed to be most sensitive to terrestrial areas. A correlation matrix was examined to determine the dependency of these six available channels on each other. Based on this correlation matrix, there were very strong correlations between Channels 4 and 5 ( $R = 0.938$ ), and Channels 6 and 7 ( $R = 0.965$ ). Therefore Channels 4 and 6 were eliminated and only four channels were chosen for analysis. These channels were 3, 5, 7, and 10. The peak wavelengths and sensing ranges for these channels are shown in Table 1.

### 3.2.4 Sample Site Location

The 29 water quality sampling sites were located in the OCS data coordinate system by applying a coordinate transformation equation between the Universal Transverse Mercator (UTM) ground coordinate system and the OCS scanner coordinate system. The transformation was based on a second-order linear regression equation. To develop this transformation equation, a network of ground point coordinates was located on the UTM System from the 7½ minute USGS topographic quadrangle maps covering the study area. Their corresponding scanner coordinates in the OCS system were also located and extracted from the OCS data. After the regression equation was developed, the UTM coordinates of the 29 sample sites were extracted from the USGS quadrangles. These UTM coordinates of the sample sites were input to the coordinate transformation equation, and the coordinates of the sample sites in the OCS coordinate system were predicted. In this way, OCS spectral data corresponding to the sample sites could be extracted from the disk file, and then related to the water quality parameters measured by the sample boats.

### 3.2.5 Spectral Data Extraction at Each Sample Site

To insure proper correspondence (or registration) of the spectral data to the sample sites, the radiance

Table 1. Peak wavelength and ranges for the four OCS channels used in this study and wavelength ranges for the four Landsat MSS bands.

|                | Peak Wavelength | Wavelength range in $\mu\text{m}$ |
|----------------|-----------------|-----------------------------------|
| OCS Channel 3  | .506            | .475 - .530                       |
| OCS Channel 5  | .586            | .550 - .610                       |
| OCS Channel 7  | .667            | .645 - .690                       |
| OCS Channel 10 | .778            | .745 - .800                       |
| Landsat Band 4 | -               | .5 - .6                           |
| Landsat Band 5 | -               | .6 - .7                           |
| Landsat Band 6 | -               | .7 - .8                           |
| Landsat Band 7 | -               | .8 - 1.10                         |

values for a nine-pixel block cell surrounding each predicted sample site were extracted from OCS Channels 3, 5, 7 and 10.

#### 3.2.6 Cell Mean Radiance Value Calculation

The average (mean) radiance value of the nine pixel cell encompassing each sample site was computed. These average cell values were used as independent variables in the regression models described below.

### 3.3 Development of Regression Models for Estimating Water Quality Parameters from OCS Data

A number of statistical models were examined for determining the best relationships between each water quality parameter and the mean radiance values generated for Channels 3, 5, 7 and 10, as well as a number of numerical functions of these channels. Based on the evaluation of correlation coefficients (R), "F" values, and the significance levels of these "F" values, the best fit for each one of the four water quality parameters was determined. These models are presented and discussed in Section 4.0.

### 3.4 Acquisition and Analysis of Landsat Multispectral Scanner Data

The Landsat-2 computer compatible Tapes (CCT) for September 1978 were obtained from the EROS Data Center in Sioux Falls, South Dakota. The following procedure was used in processing and analyzing the Landsat CCT's.

#### 3.4.1 Data Reformatting

The Landsat CCT's were reformatted to a format compatible with the Remote Sensing Research Program (RSRP) data processing system.



#### 3.4.2 Bad Data Rectification

Malfunctioning of the Landsat Multispectral Scanner at the time of data acquisition, caused a number of bad data lines. These were replaced in each instance by averaged values of the data from the lines above and below the bad data line. The correction was applied to each pixel along the bad data line.

#### 3.4.3 Landsat Band Selection

All four Landsat MSS bands (4, 5, 6, and 7) were examined for the development of regression models.

#### 3.4.4 Sample Site Location

All of the water quality sampling sites were located in the Landsat Coordinate System by applying a coordinate transformation equation between the Universal Transverse Mercator (UTM) coordinate system and the Landsat coordinate system. This transformation was based on a second order linear regression equation. To develop this transformation equation, a number of ground point coordinates were located on the UTM system from USGS maps and on their corresponding Landsat coordinates. A regression model was fit to these two sets of data: 1) the UTM coordinates; and 2) the Landsat-based coordinates. Once the regression model was determined, the UTM coordinates of the 29 sample sites were extracted from the USGS maps. These UTM coordinates of the sample sites were used as inputs to the coordinate transformation equation, and the corresponding Landsat coordinates for the 29 sample sites were calculated. This facilitated our locating the water quality sampling sites on the Landsat data.

#### 3.4.5 Spectral Data Extraction at Each Sample Site

In order to determine the correct correspondence of the Landsat spectral data to the sample sites col-

lected from boats, the radiance values for a nine-pixel block cell (3 pixels by 3 pixels) surrounding each predicted sample site were extracted from Landsat data as was done with the OCS data.

#### 3.4.6 Cell Mean Radiance Value Calculation

The average (mean) radiance values in all 4 bands of Landsat MSS data for the nine-pixel cell encompassing each sample site were computed. The average cell values were used as independent variables in the regression models described below.

#### 3.5 Development of Regression Models for Estimating Water Quality Parameters from Landsat MSS Data

Statistical models were examined for determining the best relationships between each water quality parameter and the mean radiance values computed from Landsat bands 4, 5, 6, and 7, as well as their ratios and other combinations. Based on the evaluation of correlation coefficients (R), "F" values, and the significance levels of these "F" values, the best fit for each one of the water quality parameters was determined. The Results section includes these models.

#### 3.6 Applications of Regression Models Based on the OCS or Landsat Data to the Entire Study Area

The regression models, developed between (1) the water quality measurements from boats for 29 sample sites, and (2) the mean radiance values as obtained from (a) the OCS data and (b) the Landsat data, were extended to the entire study area for mapping the desired water quality parameters. The extension of these models to the entire study area was accomplished by using a simple linear discriminant function. By applying this function to each pixel in the study area and then grouping each continuous water quality variable into discrete classes, the classification was accomplished. These discriminant functions were applied to the OCS and Landsat data to produce the water quality

maps, based on the OCS and Landsat data, respectively. The results of these classifications were produced in color-coded maps for the water quality parameters of interest. Section 4.0 of this report includes these color-coded maps.

#### 4.0 RESULTS

As the OCS data contained a number of dropout regions, we developed algorithms to replace these dropouts with new data. These procedures were discussed in Section 3.2.2. As an example, the data in Channel 10 before and after rectification of the dropouts are shown in Figures 2 and 3 respectively.

Based on the correlation matrix discussed in Section 3.2.3, only Channels 3, 5, 7 and 10 were selected for analysis. The peak wavelength and sensing range for these channels are shown in Table 1. The best fit regression models, for mapping water quality parameters from Landsat data, were based on all four bands of Landsat data. The wavelength range for these bands are also shown in Table 1. The Landsat raw data after rectification for bad data lines is shown in Figure 4.

The results of the laboratory analysis for 29 water quality sample sites are shown in Table 2.

Based on the statistical analysis, the following models were selected to represent the relationship between the water quality measurements obtained from boats and the mean radiance values obtained from the OCS and Landsat (MSS) data.

##### 4.1 Regression Models Based on the OCS Data

###### 4.1.1 Salinity Model

$$y_{EC} = a + b/x_{10} + c/(x_{10})^{1/2} + d/(x_{10})^2, \text{ where}$$

$y_{EC}$  = salinity expressed in percent.

▲ N

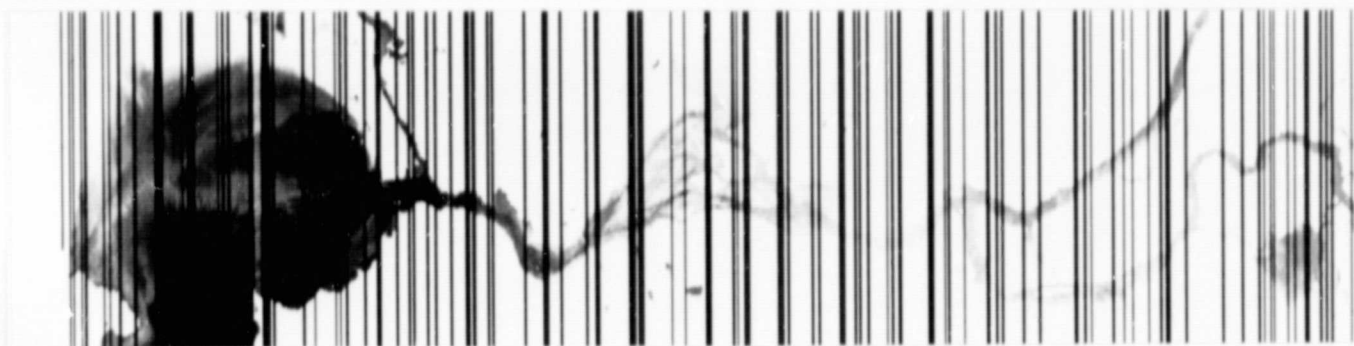


Figure 2. Display of digital OCS data in Channel 10 prior to rectification of the dropout regions.

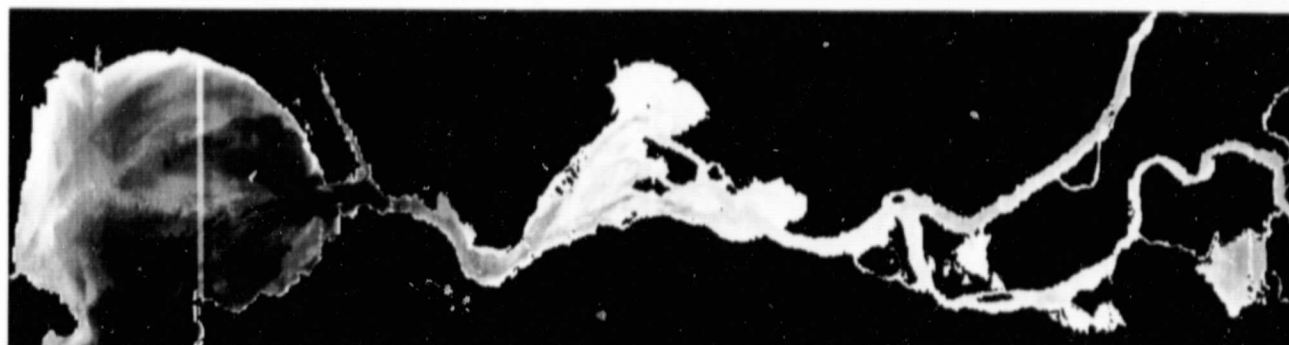


Figure 3. Display of digital OCS data in Channel 10 after rectification of the dropout regions and masking.

▲ N



Figure 4. Landsat raw data color composite of Bands 4, 5, and 7 of the study area after rectifying the bad data lines.

ORIGINAL PAGE IS  
OF POOR QUALITY

Table 2. The results of laboratory analysis for water quality samples collected on September 14, 1978.

| Sample Site # | Suspended Solids mg/l | Turbidity, mg/l SiO <sub>2</sub> | Salinity, % | Chlorophyll, mg/l |
|---------------|-----------------------|----------------------------------|-------------|-------------------|
| 1             | 29.8                  | 13.0                             | 22.0        | .0038             |
| 2             | 37.4                  | 23.0                             | 23.0        | .0044             |
| 3             | 39.4                  | 20.0                             | 18.0        | .0040             |
| 4             | 36.2                  | 18.0                             | 19.0        | .0051             |
| 5             | 44.4                  | 14.0                             | 15.0        | .0062             |
| 6             | 28.9                  | 21.0                             | 16.0        | .0138             |
| 7             | 47.1                  | 43.0                             | 12.0        | .0201             |
| 8             | -                     | 44.0                             | 10.0        | .0451             |
| 9             | 65.4                  | 41.0                             | 10.5        | .0520             |
| 10            | 69.8                  | 58.0                             | 6.0         |                   |
| 11            | 67.9                  | 41.0                             | 3.0         |                   |
| 12            | 73.0                  | 53.0                             | 4.5         |                   |
| 13            | 64.9                  | 50.0                             | 3.0         |                   |
| 14            | 69.3                  | 50.0                             | 3.0         |                   |
| 15            | 75.6                  | 47.0                             | 1.0         |                   |
| 16            | 74.5                  | 50.0                             | 1.5         |                   |
| 17            | 43.1                  | 41.0                             | 1.5         |                   |
| 18            | 69.2                  | 47.0                             | 0.0         |                   |
| 19            | 56.4                  | 41.0                             | 0.0         |                   |
| 20            | 53.5                  | 37.0                             | 0.0         |                   |
| 21            | 24.5                  | 41.0                             | 1.0         |                   |
| 22            | 80.0                  | 53.0                             | 1.5         |                   |
| 23            | 46.2                  | 52.0                             | 1.0         |                   |
| 24            | 46.0                  | 45.0                             | 0.0         |                   |
| 25            | 45.0                  | 37.0                             | 0.0         |                   |
| 26            | 21.8                  | 31.0                             | 0.0         |                   |
| 27            | 29.9                  | 23.0                             | 0.0         |                   |
| 28            | 19.7                  | 18.0                             | 0.0         |                   |
| 29            | 8.1                   | 16.0                             | 0.0         |                   |

$X_{10}$  = the mean radiance value of OCS Channel 10

$a = 405.7$ ,  $b = 3597$ ,  $c = 2306$ , and  $d = -2287$ .

#### 4.1.2 Chlorophyll Model

$$y_{CH} = a + b/X_7 + cX_{10} + dX_{10}^2 \quad \text{where,}$$

$y_{CH}$  = chlorophyll concentration expressed in mg/l.

$X_7$  = the mean radiance value of OCS Channel 7

$X_{10}$  = the mean radiance value of OCS Channel 10

$a = 0.2919$ ,  $b = 0.8065$ ,  $c = 0.09512$  and  $d = 0.009270$

#### 4.1.3 Suspended Solids Model

$$y_{SS} = a + b/X_3 + c/X_7 + dX_3 \quad \text{where,}$$

$y_{SS}$  = suspended solids, expressed in mg/l.

$X_3$  = the mean radiance value of OCS Channel 3

$X_7$  = the mean radiance value of OCS Channel 7

$a = 564.1$ ,  $b = 609.9$ ,  $c = -1694$ , and  $d = -32.62$ .

#### 4.1.4 Turbidity Model

$$y_T = a + bX_3 + c/X_3 + dX_{10} + e/X_{10} \quad \text{where,}$$

$y_T$  = turbidity, expressed in mg/l  $SiO_2$

$X_3$  = the mean radiance value of OCS Channel 3

$X_{10}$  = the mean radiance value of OCS Channel 10

$a = 1357$ ,  $b = -59.33$ ,  $c = -7008$ ,  $d = 3.417$  and

$e = 163.9$

## 4.2 Regression Models Based on Landsat MSS Data

### 4.2.1 Salinity Model

$$y_{EC} = a + bX_4 + cX_6 + dX_7 \quad \text{where,}$$

$y_{EC}$  = salinity expressed in percent

$X_4$  = the mean radiance value of Landsat Band 4

$X_6$  = the mean radiance value of Landsat Band 6

$X_7$  = the mean radiance value of Landsat Band 7

$a = 59.96$ ,  $b = -1.228$ ,  $c = -3.004$ , and  $d = 8.981$

### 4.2.2 Chlorophyll Model

$$y_{CH} = a + bX_4 + cX_5 + dX_7 \quad \text{where,}$$

$y_{CH}$  = chlorophyll concentration expressed in mg/l.

$X_4$  = the mean radiance value of Landsat Band 4

$X_5$  = the mean radiance value of Landsat Band 5

$X_7$  = the mean radiance value of Landsat Band 7

$a = 0.285$ ,  $b = -0.0225$ ,  $c = 0.00820$ , and  $d = 0.0287$

### 4.2.3 Suspended Solids Model

$$y_{SS} = a + b(X_6)^{1/2} + \frac{c}{(X_7)^2} + d(X_5)^{1/3}$$

$y_{SS}$  = suspended solids expressed in mg/l

$X_5$  = the mean radiance value of Landsat Band 5

$X_6$  = the mean radiance value of Landsat Band 6

$X_7$  = the mean radiance value of Landsat Band 7

$a = 399.850$ ,  $b = 136.787$ ,  $c = -0.0115$ , and  $d = -321.630$



#### 4 2.4 Turbidity Model

$$y_T = 12.90 + e (a + b \cdot n X_4 - 17.4) + c \cdot n X_5 - 14.32 \\ + d \cdot n X_6 - 4.88 )$$

$y_T$  = turbidity expressed in mg/l  $SiO_2$

$X_4$  = the mean radiance value of Landsat Band 4

$X_5$  = the mean radiance value of Landsat Band 5

$X_6$  = the mean radiance value of Landsat Band 6

$a = 1.053$ ,  $b = 0.613$ ,  $c = 0.529$ , and  $d = 0.860$ .

To prepare the color-coded maps of estimated water quality parameters, the regression models established between the 29 water quality measurements from boats and remote sensing data (the OCS data and Landsat data) were extended to the entire study area, using a simple linear discriminant function. Applications of these functions resulted in a series of maps which were then color-coded to represent the four water quality parameters. The color-coded maps of the entire study area for salinity, chlorophyll concentration, suspended solids and turbidity (based on the OCS data) are shown in Figures 5, 6, 7, and 8 and for salinity, chlorophyll concentration, suspended solids, and turbidity (based on Landsat MSS data) are shown in Figures 9, 10, 11, and 12 respectively.

#### 5.0 DISCUSSION

The correlation coefficients (R), measuring the closeness with which the regression models fit the water quality measurements, and the "F" values for both OCS-based models are shown in Table 3. In general, the values

LEGEND

| <u>Color</u>  | <u>Salinity, ‰</u> |
|---------------|--------------------|
| Black         | 0.0                |
| Dark Blue     | 0.1 - 0.9          |
| Blue          | 1.0 - 1.9          |
| Light Blue    | 2.0 - 3.9          |
| Green         | 4.0 - 5.9          |
| Yellow        | 6.0 - 7.9          |
| Yellow-orange | 8.0 - 9.9          |
| Orange        | 10.0 - 11.9        |
| Light Red     | 12.0 - 13.9        |
| Red           | 14.0 - 15.9        |
| Brown-red     | 16.0 - 22.9        |



Figure 5. Salinity Distribution as derived from OCS data for the Delta region; San Pablo Bay is on left.

ORIGINAL PAGE IS  
OF POOR QUALITY

| Color         | Chlorophyll,<br>mg/l |
|---------------|----------------------|
| Black         | .000                 |
| Dark Blue     | .001 - .004          |
| Blue          | .005 - .009          |
| Light Blue    | .010 - .014          |
| Green         | .015 - .019          |
| Yellow        | .020 - .024          |
| Yellow-orange | .025 - .029          |
| Orange        | .030 - .034          |
| Light Red     | .035 - .039          |
| Red           | .040 - .044          |
| Brown-red     | .045 - .084          |

▲ N

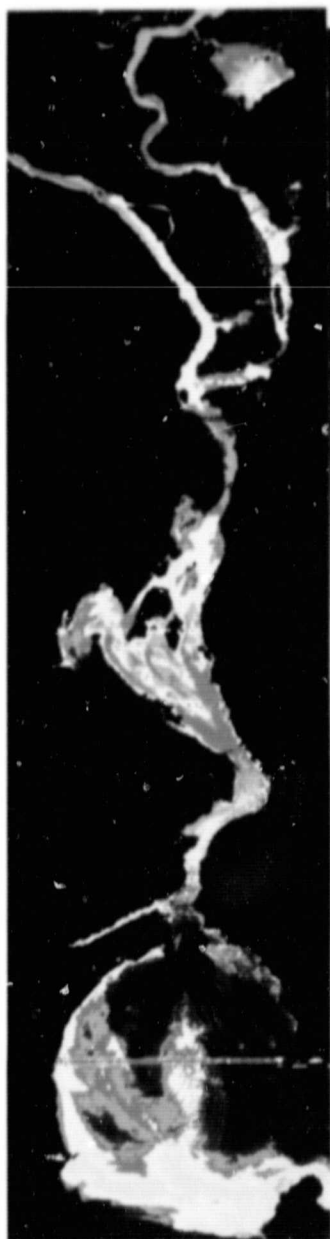


Figure 6. Chlorophyll distribution as derived from OCS data for the Delta region; San Pablo Bay is on left.

ORIGINAL PAGE IS  
OF POOR QUALITY

LEGEND

| <u>Color</u>  | <u>Suspended Solids,<br/>mg/l</u> |
|---------------|-----------------------------------|
| Black         | 0.0                               |
| Dark Blue     | 0.1 - 9.9                         |
| Blue          | 10.0 - 19.9                       |
| Light Blue    | 20.0 - 29.9                       |
| Green         | 30.0 - 39.9                       |
| Yellow        | 40.0 - 49.9                       |
| Yellow-orange | 50.0 - 59.9                       |
| Orange        | 60.0 - 69.9                       |
| Light Red     | 70.0 - 79.9                       |
| Red           | 80.0 - 89.9                       |
| Brown-red     | 90.0 - 99.9                       |

A N

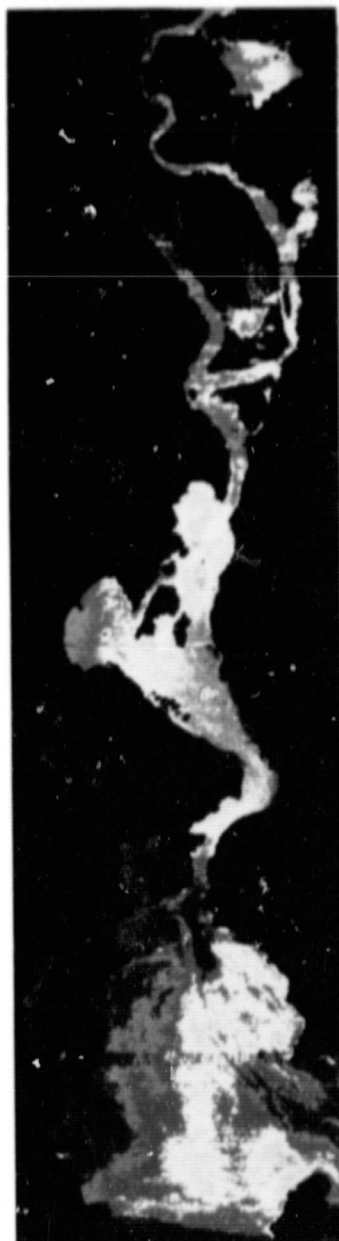


Figure 7. Suspended solids distribution as derived from OCS data for the Delta region; San Pablo Bay is on left.

LEGEND

| <u>Color</u> | <u>Turbidity, mg/l</u><br><u>SiO<sub>2</sub></u> |
|--------------|--|
| Black        | 0.0  |
| Dark Blue    | 0.1 - 9.9  |
| Blue         | 10.0 - 19.9                                      |
| Light Blue   | 20.0 - 29.9                                      |
| Green        | 30.0 - 39.9                                      |
| Yellow       | 40.0 - 49.9                                      |
| Orange       | 50.0 - 59.9                                      |
| Red          | 60.0 - 69.9                                      |

▲ N

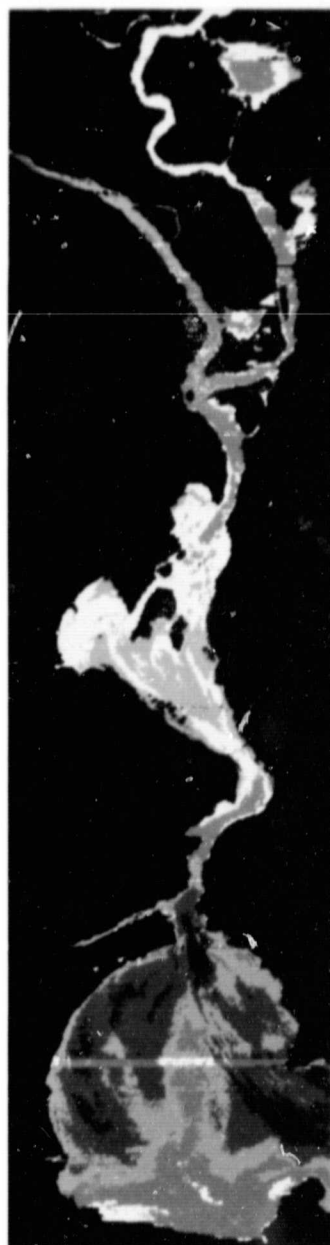


Figure 8. Turbidity distribution as derived from OCS data for the Delta region; San Pablo Bay is on left.

ORIGINAL PAGE IS  
OF POOR QUALITY

| <u>Color</u>  | <u>Salinity, ‰</u> |
|---------------|--------------------|
| Black         | 0.0                |
| Dark Blue     | 0.1 - 0.9          |
| Blue          | 1.0 - 1.9          |
| Light Blue    | 2.0 - 3.9          |
| Green         | 4.0 - 5.9          |
| Light Green   | 6.0 - 7.9          |
| Yellow        | 8.0 - 9.9          |
| Yellow-orange | 10.0 - 11.9        |
| Orange        | 12.0 - 13.9        |
| Light Red     | 14.0 - 15.9        |
| Red           | 16.0 - 17.9        |
| Brown         | 18.0 - 25          |

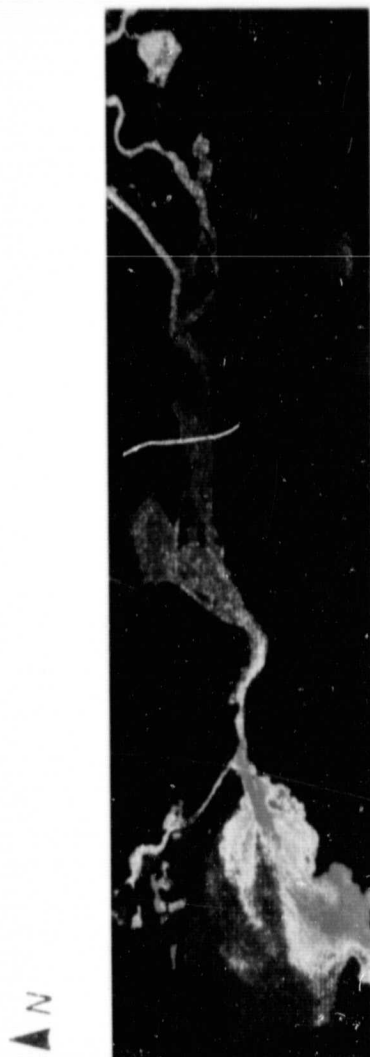


Figure 9. Salinity distribution as derived from the enhanced Landsat MSS data for the Delta region; San Pablo Bay is on left.

LEGEND

| <u>Color</u>  | <u>Chlorophyll, mg/l</u> |
|---------------|--------------------------|
| Black         | 0.000                    |
| Dark Blue     | 0.001 - .004             |
| Blue          | .005 - .009              |
| Light Blue    | .010 - .014              |
| Green         | .015 - .019              |
| Light Green   | .020 - .024              |
| Yellow        | .025 - .029              |
| Yellow-orange | .030 - .034              |
| Orange        | .035 - .039              |
| Light Red     | .040 - .045              |
| Red           | .045 - .049              |
| Brown         | .50 - .100               |

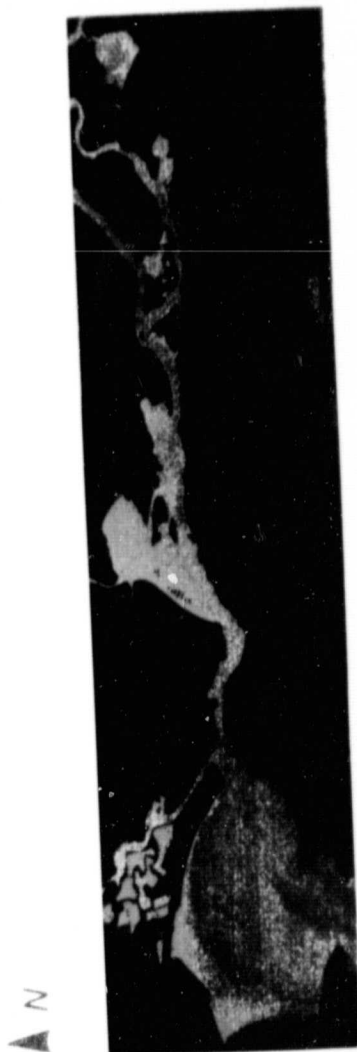


Figure 10. Chlorophyll distribution as derived from the enhanced Landsat MSS data for the Delta region; San Pablo Bay is on left.

LEGEND

| <u>Color</u>  | <u>Suspended Solids,<br/>mg/l</u> |
|---------------|-----------------------------------|
| Black         | 0.0                               |
| Dark Blue     | 0.1 - 9.9                         |
| Blue          | 10.0 - 19.9                       |
| Light Blue    | 20.0 - 29.9                       |
| Green         | 30.0 - 39.9                       |
| Light Green   | 40.0 - 49.9                       |
| Yellow        | 50.0 - 59.9                       |
| Yellow-orange | 60.0 - 69.9                       |
| Orange        | 70.0 - 79.9                       |
| Light Red     | 80.0 - 89.9                       |
| Red           | 90.0 - 100                        |

▲ N

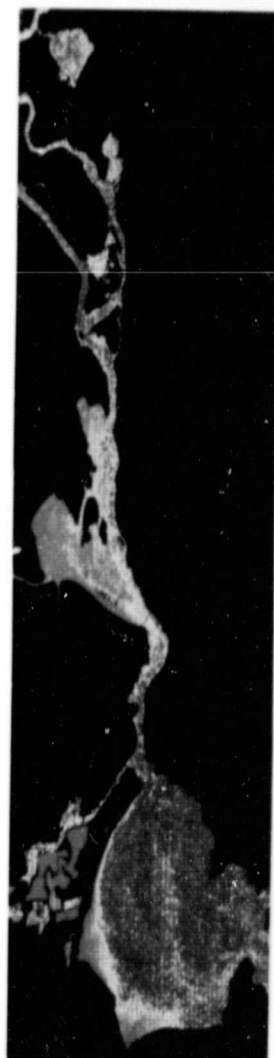
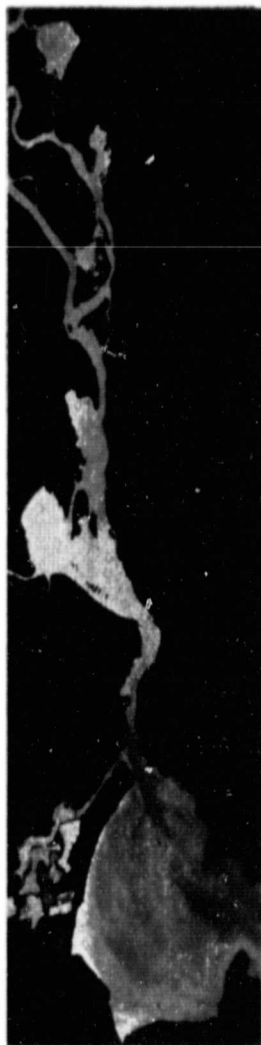


Figure 11. Suspended solids distribution as derived from the enhanced Landsat MSS data for the Delta region; San Pablo Bay is on left.



▲ N



LEGEND

| <u>Color</u>  | <u>Turbidity, mg/l</u><br><u>SiO<sub>2</sub></u> |
|---------------|--|
| Black         | 0.0  |
| Dark Blue     | 0.1 - 9.9  |
| Blue          | 10.0 - 19.9                                      |
| Light Blue    | 20.0 - 29.9                                      |
| Green         | 30.0 - 39.9                                      |
| Light Green   | 40.0 - 49.9                                      |
| Yellow        | 50.0 - 59.9                                      |
| Yellow-orange | 60.0 - 69.9                                      |
| Orange        | 70.0 - 79.9                                      |
| Light Red     | 80.0 - 89.9                                      |
| Red           | 90.0 - 100                                       |

Figure 12. Turbidity distribution as derived from the enhanced Landsat MSS data for the Delta region; San Pablo Bay is on left.

**Table 3.** Correlation Coefficients (R) and "F" values relating remotely sensed data to "ground truth" for the four water quality parameters estimated using the regression models on Ocean Color Scanner (OCS) and Landsat data.

| Water Quality Parameter | R     |         | F*   |         |
|-------------------------|-------|---------|------|---------|
|                         | OCS   | Landsat | OCS  | Landsat |
| Salinity                | 0.948 | .863    | 73.5 | 24.3    |
| Chlorophyll             | 0.934 | .905    | 11.4 | 59.2    |
| Suspended Solids        | 0.609 | .674    | 4.9  | 6.9     |
| Turbidity               | 0.791 | .907    | 10.0 | 60.2    |

of the correlation coefficients may be summarized as:

1) high for chlorophyll concentrations based on the OCS data and also based on Landsat data; 2) high for salinity based on the OCS data; 3) medium for salinity based on Landsat data; 4) medium for turbidity based on the OCS data; 5) high for turbidity based on Landsat data; and 6) relatively low for suspended solids based on the OCS data and also based on Landsat data. This indicates that: 1) chlorophyll concentrations can be estimated by either the OCS or Landsat data with approximately equal accuracy; 2) salinity can be best estimated by the OCS data; 3) turbidity can be best estimated by Landsat data; and 4) neither the OCS data nor the Landsat data provide a reliable basis for estimating suspended solids.

All of the "F" values were significant at the 0.01 level of significance. This indicates that variations in spectral response account for a significant portion of the variations in water quality parameters.

In all of these color-coded maps, the values of the given water quality parameters increase in accordance with the following sequence of colors:

dark blue, blue, green, yellow, orange, red, brown  
(low concentration) —————> (high concentration)

The analysis of the chlorophyll, suspended solids, and turbidity maps indicates the existence of a region with high chlorophyll content, high suspended solids, and high turbidity. This region is referred to as a "region of high biological activity" in this report and is shown

in red and brown colors in Figures 6, 7, 8, 10, 11, and 12. To some scientists this region has also become known as the "Entrapment Zone."

The salinity values in the study area increased constantly as the San Pablo Bay was being approached from the Delta. The lower salinity values were observed in the west side of the San Pablo Bay. This was due to the fresh water in-flow from Napa and Sonoma Rivers to the Bay in that region.

## 6.0 CONCLUSION

Based on the results and the associated analyses that were made of the various kinds of imagery, the following conclusions are indicated:

1. Areas of high biological activity were clearly discernible on suitably enhanced digital data from the OCS and also from the Landsat MSS. This area was characterized by high turbidity, high suspended solids, and high chlorophyll concentration.
2. It was virtually impossible, at least within this test site, to locate such areas on aerial photography of the highest quality that had been taken with either conventional color or infrared-sensitive color films.
3. Consistent with our findings, many investigators from different parts of the world, through the use of conventional ground survey techniques, have reported the region of

high turbidity and high suspended solids to be a persistent feature of moderately stratified estuaries.

4. Comparison of the results based on the OCS and Landsat data indicated that:
  - a. Chlorophyll concentrations can be estimated by either the OCS or Landsat data with approximately equal accuracy.
  - b. Salinity can be best estimated by the OCS data.
  - c. Turbidity can be best estimated by Landsat data; and
  - d. Neither the OCS data nor the Landsat data provides reliable basis for estimating suspended solids.
5. Although, in a few other instances, remote sensing data derived from multi-spectral scanners has been successfully used for the purpose of water quality mapping, it is believed that the present study constitutes the first concerted effort to use remote sensing to locate the estuarine region of highest biological activity and to analyze such associated parameters as turbidity, suspended solids, chlorophyll concentration and salinity.
6. It is deemed especially noteworthy that in the present study remote sensing data derived from the Ocean Color Scanner and/or the Landsat

Multispectral Scanner proved highly useful in mapping water quality parameters associated with determining both size and migration of the "region of high biological activity" in the San Francisco Bay and its associated Delta.

#### ACKNOWLEDGEMENTS

The research documented in this report was supported jointly by the National Aeronautics and Space Administration (NASA) - Goddard Space Flight Center Grant NSG 5256 and by the University of California Water Resources Center, Davis, as part of Project UCAL-WRC-W561.

The investigators of the research effort wish to express their gratitude to the research, technical and administrative staff of both the Remote Sensing Research Program, Space Sciences Laboratory, University of California, Berkeley, and the Department of Land, Air and Water Resources, University of California, Davis for directing significant time and expertise to this project.

## REFERENCES

- Arthur, J.F. 1975. Preliminary Studies on the Entrapment of Suspended Materials in Suisun Bay, San Francisco Bay-Delta Estuary, IN R. L. Brown (ed.), Proceedings of a Workshop on Algae Nutrient Relationships in the San Francisco Bay and Delta, San Francisco Bay and Estuarine Association, pp. 17-36.
- Arthur, J.F. 1977. The null zone: 1976 measurements and possible ecological significance. Presented at winter meeting, San Francisco Bay and Estuarine Association.
- Barker, J.L. 1975. Monitoring Water Quality from Landsat. NASA/GSFS, National Technical Information Service N76-11543.
- Brooks, D.J. 1975. Landsat Measures of Water Quality. Photogrammetric Engineering and Remote Sensing, Vol. 41 (10): 1269-1272.
- Draeger, W.C., A.S. Benson, and L.A. Johnson. 1974. Usefulness of remote sensing techniques for the environmental monitoring of the Sacramento-San Joaquin Delta. Final Report, California Dept. Water Resources Contract #B51010. School of Forestry and Conservation, University of California, Berkeley, 51p.
- Glandeaud, L. 1959. Le Mouvement des Sediments et al Formation des Bancs, Seuils et Mouilles Dans la Garonne et l'estuarie de la Girond. Int. Assoc. Sci. Hydrology, Washington, Prov., v. 1, Comm. Potamology, Question 3, Rept. 6, 14 pp.
- Inglis, C.C. and J.H. Allen. 1957. The Regimen of the Thames Estuary as Affected by Currents, Salinities, and River Flow. Inst. Civil Engineers Proc., v. 7, pp. 827-878; disc. v. 8, pp. 437-439.
- Johnson, R.W. 1976. Quantitative Sediment Mapping from Remotely Sensed Multispectral Data. Proc, Fourth Annual Remote Sensing of Earth Resources Conference, Tullahoma, Tennessee.

- Khorram, S. 1979. Remote Sensing Analysis of Water Quality in the San Francisco Bay Delta. Proc. 13th International Symposium on Remote Sensing of Environment. Environmental Research Institute of Michigan, Ann Arbor, Michigan.
- McKee, J.B. and R.H. Rogers. 1976. Water Quality Map of Saginaw Bay from Computer Processing of Landsat-2 data. Spec. Report. NASA-Goddard Space Flight Center, Greenbelt, Maryland, 5p.
- Meade, R.H. 1967. Relations Between Suspended Matter and Salinity in Estuaries of the Atlantic Seaboard. U.S.A. Internat. Assoc. Sci. Hydrology, Pub. 78, Gen. Assembly, Bern, v 4, pp. 96-109.
- Meade, R.H. 1972. Transport and Deposition of Sediments in Estuaries. Mem. Geol. Soc. Am. No. 133, pp. 91-120.
- Peterson, D.H., T.J. Conomos, W.W. Broakow, and P.C. Doherty. 1975. Location of the Non-Tidal Current Null Zone in Northern San Francisco Bay. Estuarine and Coastal Marine Science 3, pp. 1-11.
- Postma, H. 1967. Sediment Transport and Sedimentation in the Estuarine Environment. IN G.H. Lauff (ed.), Estuaries. Am. Assoc. Adv. Sci. Pub. 83, pp. 158-179.
- Rogers, R.H., L.E. Reed, and V.E. Smith. 1975. Computer Mapping of Turbidity and Circulation Patterns in Saginaw Bay, Michigan (Lake Huron) from ERTS data. Proc. ASP-ACSM Convention, Washington, D.C., 15p.
- Scherz, J.P., D.R. Crane, and R.H. Rogers. 1975. Classifying and Monitoring Water Quality by use of Satellite Imagery. Proc. International Conference on Environmental Sensing and Assessment, Las Vegas, Nevada, 24p.
- Schubel, J.R. 1968. Turbidity Maximum of the Northern Chesapeake Bay. Science 161, pp. 1013 - 1015.